Fuel 187 (2017) 128–136

Contents lists available at ScienceDirect

Fuel

journal homepage: www.elsevier.com/locate/fuel

Full Length Article

Catalytic reforming of toluene and naphthalene (model tar) by char supported nickel catalyst

Kezhen Qian, Ajay Kumar *

Department of Biosystems and Agricultural Engineering, Oklahoma State University, Stillwater, OK, United States

HIGHLIGHTS

- Char supported nickel catalysts were prepared for model tar reforming.
- Effect of nickel precursors and hydrazine on catalysts' performance were studied.
- Char with nickel nitrate precursor was more effective than char with nickel acetate.
- The presence of naphthalene affected reforming of toluene.

ARTICLE INFO

Article history:
Received 10 May 2016
Received in revised form 22 August 2016
Accepted 12 September 2016

Keywords:
Char
Catalyst
Tar reforming
Gasification

ABSTRACT

The purpose of this study was to utilize gasification derived char as a catalyst support for tar removal. Red cedar char collected from downdraft bed gasification was chemically activated into activated carbon and impregnated with nickel acetate and nickel nitrate. The effects of nickel salts precursor, nitric acid treatment of support and reduction of nickel in hydrazine medium on catalyst performance were studied. It was found nickel nitrate was a better nickel precursor than nickel acetate for preparation of char supported nickel catalyst. The catalyst impregnated with nickel nitrate was found more active in steam reforming of toluene than the catalyst impregnated with nickel acetate. TEM results indicated that nickel particle size of the catalyst impregnated with nickel nitrate was much smaller than that of the catalyst impregnated with nickel acetate. Toluene showed higher removal efficiency than naphthalene. The presence of naphthalene decreased the toluene removal.

1. Introduction

Gasification, a biomass thermochemical conversion technology, converts biomass into synthesis gas (syngas), a mixture of primarily carbon monoxide, carbon dioxide and hydrogen. The produced syngas can further be used as a feedstock for hydrocarbon fuels production through the Fischer–Tropsch synthesis (FTS) process, which produces hydrocarbons of different lengths. Syngas can also be used as an alternative to natural gas fuel for hydrogen or power production. However, biomass-generated syngas cannot be used directly because it contains high concentration of tars which are a mixture of several aromatic compounds. The components of biomass tars can be categorized into five classes: undetectable, heterocyclic, light aromatic hydrocarbons (LAH), light polyaromatic hydrocarbons (LPAH) and heavy polyaromatic hydrocarbons (HPAH) [1].

The tars must be removed prior to utilization of syngas [2,3] because tars cause a lot of equipment problems, such as condensation on facility leading to fouling [3]. The environmental legislation also requires removal of toxic aromatic compounds from syngas. Wet scrubbing, catalytic conditioning and high temperature thermal cracking are three major syngas cleaning methods. Catalytic conditioning is of the most promising because of its high conditioning efficiency. In addition, catalytic conditioning of syngas tars can increase syngas H_2/CO [1,4,5] that is, typically, inadequate (<1) for the FTS (about 2.0) and other syngas conversions [6].

Recently, biochar, one of the byproducts of biomass gasification, was reported as a potential catalyst for tar removal [7]. The catalytic activity of char for tar elimination can be related to its high pore size, surface area, and ash/mineral content. Char can also be activated into activated carbon and used as a support for preparing metal catalysts [8,9]. When used as a catalyst support, activated carbon has unique properties, such as its stability in both acidic

* Corresponding author at: 228 Agricultural Hall, Biosystems and Agricultural Department, Biobased Products and Energy Center, Oklahoma State University, Stillwater, OK 74078, United States.
E-mail address: ajay.kumar@okstate.edu (A. Kumar).

http://dx.doi.org/10.1016/j.fuel.2016.09.043
0016-2361/

and basic media, the possibility of easy recovery of precious metals supported on it and the possibility of tailoring both its textural and surface chemical properties [10,11].

Pretreatments to the carbon support can significantly affect the properties and performance of the carbon-based catalysts. High surface area, acid groups and oxygen-containing functional groups on the surface play an important role in catalyst reactivity of biochar. The metal dispersion ratio and metal–carbon interactions also affect the reactivity of carbon supported metal catalysts. Several studies have confirmed that pre-treatments of activated carbon increase metal dispersion ratio, support surface area and surface functional group, thus, influence its reactivity [12,13]. Pre-treatment includes acid treatment of carbon with various acids (H_2SO_4, HNO_3) and reducing agents (hydrazine and $NaBH_4$). Acid treatment can increase surface oxygenated groups on the activated carbon, and thus increase its catalytic activity [12,14–16]. Aksoylu et al. [12] studied the effect of HNO_3 treatment on Pt/carbon catalyst performance in the benzene hydrogenation reaction. The results showed that HNO_3 treatments not only led to increase in oxygen bearing groups on the exterior and interior surfaces of the activated carbon, but also enhanced dispersion of Pt. The catalyst activity test showed that the treated catalyst exhibited higher efficiency as compared to the untreated catalyst [14]. Besides acid treatment, hydrazine treatment has also been widely used in catalyst preparation as a reducing agent of metallic catalyst. Treating the catalyst with reducing agent produces nanoparticle metal catalyst with small average particle size and high dispersive ratio [13,17,18]. Wojcieszak et al. [13] compared the properties of hydrazine treated catalysts (reduction of nickel by aqueous hydrazine) and classically prepared catalysts (without the hydrazine treatment) and found that the hydrazine reduction process improved metal dispersion and catalyst efficiency.

Nickel based catalysts have been widely used in tar reforming [19–22]. Świerczyński et al. [23] found that the nickel based catalyst was very effective in reforming of tars. Michel et al. [20] compared performances of olivine-based catalysts for steam reforming of methylnaphthalene (MNP) as a model tar compound. The results showed that conversion efficiency of MNP to CO/H_2 with olivine alone (4%) was much lower than that with Ni/olivine (30%).

The objective of this study was to develop novel char based catalysts. Red cedar-derived char was used as a precursor for making activated carbon support material for nickel. The effects of pretreatment method and precursor on the catalytic performances were studied: the first type of catalyst was prepared by mild oxidation of activated carbon (support) with nitric acid and reduction of impregnated nickel acetate or nickel nitrate with hydrogen; the second type of catalyst was prepared by reduction of nickel acetate with hydrazine. The properties of char based catalysts were evaluated using TEM, XRD and N_2 isotherms, and the catalysts' performances were tested in steam reforming of toluene and naphthalene (model tar compounds). Toluene was used as light monoaromatic model tar compound. Naphthalene was used as light polyaromatic model tar compound because high molecular weight compounds, such as naphthalene, are difficult to crack and have not been studied extensively.

2. Materials and methods

2.1. Materials

The char for making catalysts in this study was produced from gasification of eastern red cedar in a unique downdraft gasifier as described in previous study [24]. The resulting biochar contained 66.4% C, 1.9% H and 0.2% N on dry basis [24]. The gasification temperature was around 900 °C [24]. $Ni(NO_3)_2{\cdot}6H_2O$, $Ni(CH_3COO)_2{\cdot}4H_2O$ ($\geqslant$99.0%) and hydrazine anhydrate (50–60%) were purchased from Sigma Aldrich (St. Louis, MO, USA). The KOH was purchased from Fisher Scientific (Pittsburgh, PA, USA).

2.2. Activated carbon preparation

Chemical activation is a widely used activation method for making activated carbon [25,26]. This method uses chemicals such as KOH and NaOH as an activator to develop pores. In our study, char was mixed with KOH and soaked for 2 h. The mixture was dried in an oven overnight at 105 °C. The dried mixture was then placed in a fixed-bed tubular reactor and activated. The reactor was first heated to 300 °C and held at this temperature for 2 h to prevent carbon loss from char. For carbonization, the temperature was then raised to 800 °C and char was activated at this temperature for 1.5 h under nitrogen flow of 200 ml/min. After carbonization, the char was washed with deionized water until the pH of leaching water reached 7. The activated carbon prepared using this method contained 79.03% C, 1.92% H, and 0.51% N on dry basis.

2.3. Catalyst synthesis

The activated carbon was treated with 30 vol.% HNO_3 before loading nickel. Activated carbon was loaded in a round bottom flask equipped with a thermometer and reflux condenser. The flask was immersed in a water bath at 70 °C. The activated carbon suspension was stirred continuously using a magnetic stirrer bar. After 1.5 h acid treatment, activated char was filtered from the suspension into a funnel and washed with deionized water until pH of the filtered solution reached neutral. The acid soaked char was then dried in an oven at 105 °C overnight. The activated carbon treated with acid contained 69.18% C, 1.04% H, and 0.56% N on dry basis. The dried acid treated activated char was the wet impregnated in a solution of nickel acetate or nickel nitrate. The concentration of the nickel acetate solution was calculated before impregnation in order to achieve 10 wt.% nickel loading. The mixture was ultrasonicated for 3 h and kept in a vacuum desiccator for 16 h. The soaked samples were then dried in the oven at 105 °C and denoted as Ni-AC-N (activated char loaded with nickel nitrate) and Ni-AC-A (activated char loaded with nickel acetate).

To study the effect of hydrazine reduction on catalyst properties, Ni-AC-A was further treated with hydrazine using a method reported in literature [13]. The catalyst precursor was soaked in a 2.0 M hydrazine solution for reduction. The reduction of nickel catalyst precursor was performed in a 250 ml three necked flask that was immersed in a hot water bath. The reaction flask was fitted with a reflux condenser, a thermometer and a gas tubing for using helium to purge the air out of the flask. The mixture of nickel catalyst precursor and hydrazine solution was stirred at 80 °C for 4 h. After reduction, the catalyst was filtered and the excess hydrazine left in catalyst was washed off with deionized water. The catalyst was then dried in an oven at 105 °C before test and denoted as Ni-AC-AH.

2.4. Catalyst activity test

2.4.1. Steam reforming of toluene

The catalytic reforming tests were performed in a fixed bed reactor with a 1/2 in. inner diameter. One layer of quartz wool was kept beneath the catalyst (particle size of 0.3–0.6 mm and weight of 0.25 g) for support and one layer of quartz wool was kept above the catalyst. The catalyst was reduced in 200 ml/min hydrogen (50% hydrogen, 50% nitrogen) flow at 350 °C for 3 h before testing. During testing, 150 ml/min nitrogen controlled by mass flow controller (Burkert, Charlotte, NC, USA) was introduced into the reactor. The water and toluene were injected into evaporator by

two syringe pumps (KDS scientific, model 200, Holliston, MA, USA) and carried by nitrogen gas into the reactor. The gas pipes were heated to 250 °C to prevent tar condensation. The feeding rate of water was adjusted to achieve steam to carbon ratio of 2. Conditioning temperatures for toluene only (no naphthalene) were 600, 700 and 800 °C. The gas hourly space velocities (GHSV) were about 8000 h^{-1}. Sample was injected at about 50 min.

2.4.2. Steam reforming of naphthalene/toluene

As naphthalene is a solid at room temperature, naphthalene was used in a solution with toluene as solvent (10 wt.% of naphthalene). The water and naphthalene/toluene mixture were injected into an evaporator by syringe pumps and carried by nitrogen gas into the reactor. Because naphthalene was harder to reform, conditioning temperatures for naphthalene/toluene were set at 700, 800 and 900 °C. The steam to carbon ratio and gas hourly space velocities for naphthalene/toluene mixture were same with that for toluene. However, only Ni-AC-N was used for catalytic reforming of naphthalene/toluene mixture.

2.4.3. Tar and gas composition analysis

Concentration of reactor outlet gas (hydrogen, carbon monoxide, carbon dioxide and methane) was measured by a gas chromatograph with FID detector (Model CP-3800, Varian, Inc., Palo Alto, CA, US) and installed with a packed column (HayeSep DB). The toluene and naphthalene concentration was determined by a gas chromatograph installed with a capillary column (DB-5) and a mass spectroscopy detector (GC 7980A, MS 5975, Agilent, Santa Clara, CA, US).

The tar conversion can be defined by Eq. (1) [27]:

$$\text{Conversion } (\%) = \frac{C_{tar}^{in} - C_{tar}^{out}}{C_{tar}^{in}} \times 100 \quad (1)$$

where C_{tar}^{in} and C_{tar}^{out} were the model tar (naphthalene or toluene) molar flow rates of the inlet and outlet gases. Benzene yield as Eq. (2) [27]:

$$\text{Benzene yield } (\%) = \frac{6 \times C_{benzene}^{out}}{7C_{toluene}^{in} + 10C_{naphthalene}^{in}} \times 100 \quad (2)$$

Gas composition was calculated as Eq. (3) [27]:

$$\text{Gas composition } (\%) = \frac{\text{mole of each gas product}}{\text{total mole of gas products } (H_2 + CO + CO_2 + CH_4)} \times 100 \quad (3)$$

2.5. Catalyst characterizations

2.5.1. XRD, SEM and TEM

The morphologies of activated char supported catalysts were characterized by X-ray diffraction (XRD) and transmission electron microscopy (TEM). Particle size and crystalline phase of Ni were determined using XRD (Philips X'pert X-ray diffractometer, Westborough, MA, USA). XRD experiments were performed using Cu Kα radiation, 0.15418 nm at 40 kV and 100 mA. Diffraction data was recorded using continuous scanning at a step size of 0.02°, 0.5 s per step. The average particle size of Ni was calculated according to the Scherrer–Warren equation. The Ni dispersion was examined using transmission electron microscopy (TEM) (JEOL JEM-2100, AKISHIMA-SHI, Tokyo, Japan). TEM images were obtained by dispersing catalysts on carbon grids in isopropanol under supersonic-wave shaking. The morphologies of the activated char, fresh and used catalyst (used in reforming for 2 h) were examined by Scanning Electron Microscopy (SEM) (FEI Quanta 600, FEI Company, Hillsboro, OR, USA).

2.5.2. Surface area and Temperature-Programmed Desorption (TPD)

Surface area and pore properties (pore distribution and average pore size) of catalysts and char were measured via N_2 adsorption at −198 °C using a surface area analyzer (Autosorb-1C, Quantachrome, Boynton Beach, FL, USA). Surface area (S_{BET}) was analyzed using Brunauer–Emmett–Teller (BET) theory. Pore volumes and pore size distribution were estimated using Quenched Solid State Functional Theory (QSDFT).

TPD experiments of activated char supports were carried out in the same equipment with N_2 adsorption. Samples were first dried at 140 °C for 60 min to remove moisture under 40 ml/min helium flow. The dried sample was cooled to 100 °C before test and then heated from 100 °C to 900 °C at a heating rate of 20 °C/min. The evolved CO and CO_2 were detected by a thermal conductivity detector (TCD).

2.5.3. Fourier Transform Infrared (FTIR) analysis

Surface functional groups of char were analyzed using Fourier transform infrared spectroscopy (Nicolet FT-IR 6700, Thermo Electron Corporation, Madison, WI, USA). For each sample, 256 scans were obtained at 8 cm^{-1} resolution from 4000 to 650 cm^{-1}. Ambient air was scanned as background signal prior to scanning samples. The FTIR spectral peaks were analyzed by comparing the peak position with known peaks.

3. Results and discussion

3.1. Catalyst characterization

3.1.1. Nitrogen adsorption

Specific surface areas (S_{BET}) and pore volumes were measured using a liquid nitrogen isothermal method and listed in Table 1. Based on the results, char surface area was significantly increased by chemical activation (increased from 68 m^2/g to 1570 m^2/g). Acid treatment did not significantly reduce the surface area of the activated char. 10% nickel loading significantly decreased the surface area of the activated char (reduced about 30–40%). The char was dominated by mesopores (52 vol.%), followed by micropores (42 vol.%) with total pore volume of 0.04 cm^3/g. After activation, the total pore volume of activated char increased and so did the volume percent of micropores. More detailed pore size information was obtained from pore distribution analysis (see Fig. 1). Large quantities of micropores (<2 nm) and mesopores (2–50 nm) were detected. The mesopores were mostly composed of small mesopores (<8 nm).

Compared with acid activated char, the pore volume percent of micropores of Ni-AC-N and Ni-AC-A increased while pore volume percent of mesopores of Ni-AC-N and Ni-AC-A decreased (see Table 1). Peak corresponding to mesopores with pore diameter of 8–10 nm (Fig. 1) appeared in the activated char supports but did not appear in Ni-AC-N and Ni-AC-A. The decrease of mesopores was probably due to integration of nickel to mesopores. A similar finding was discovered by Domingogarcia et al. [9] on carbon based nickel catalyst. They found that nickel dispersion positively related to the mesopores and macropores volume of the carbon support, and concluded that only mesopores and macropores were accessible by nickel precursor.

3.1.2. TPD and FT-IR

Oxygenated functional groups on activated char were analyzed using TPD and FT-IR. Volatiles desorption occurred at different temperatures due to decomposition of various oxygenated functional groups over activated char surface. The decomposition temperatures of oxygen bearing surface groups with TPD are well studied in literatures [12,28]: the low temperature peak resulted

Table 1
Texture properties of the different activated chars and char supported Ni catalysts.

	S_{BET} (m^2/g)	V_{micro} (cm^3/g)	V_{micro} (%)	V_{meso} (cm^3/g)	V_{meso} (%)	Total pore volume (cm^3/g)	$D_{Ni,\ TEM}$ (nm)	$D_{Ni,\ XRD}$ (nm)
Raw char	68^a	0.02^a	42.85^b	0.02^a	52.38^d	0.04^a	NA	NA
AC	1570^d	0.50^c	62.50^c	0.30^d	37.50^c	0.80^c	NA	NA
Acid AC	1524^d	0.50^c	70.40^d	0.21^c	29.60^b	0.71^c	NA	NA
Ni-AC-N	965^c	0.31^b	73.80^d	0.11^b	26.20^b	0.42^b	7–13	NA
Ni-AC-A	945^c	0.30^b	75.00^d	0.10^b	25.00^b	0.40^b	15–39	18
Ni-AC-AH	1021^c	0.35^b	79.50^d	0.06^a	20.50^a	0.44^b	11–18	17
Used Ni-AC-N	265^b	0.07^a	21.80^a	0.19^c	59.37^d	0.32^b	NA	NA

"NA" means not applicable.
S_{BET}, V_{micro} and V_{meso} represent BET surface area, micropore and mesopore volume respectively.
Means followed by the same letter within a row are not significantly different ($\alpha = 0.05$).

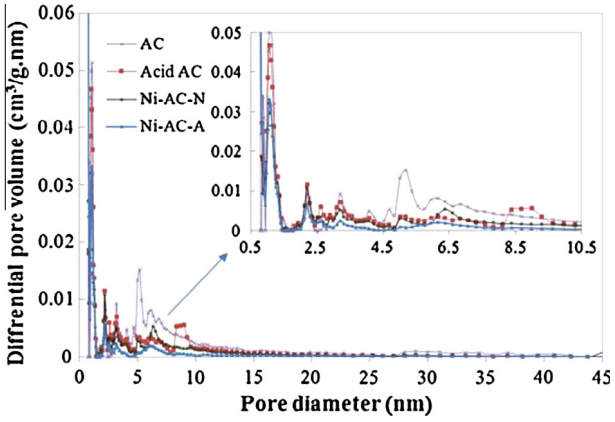

Fig. 1. Pore distribution of activated char and char supported Ni catalysts.

from decomposition of carboxylic acids (200–300 °C); the medium temperature peaks were assigned to lactones (190–650 °C); higher temperature decompositions were assigned to carboxylic anhydrides, carbonyl, phenols, ethers, carbonyls and quinone groups (700–1000 °C). As seen in Fig. 2, peaks were observed in all temperature regions for both activated char and acid treated activated char, indicating that activated char and acid treated activated char contained multiple oxygen functional groups. The peaks of acid treated activated char were higher than peaks of raw activated char, indicating that acid treatment increased the quantity of surface oxygen functional groups on activated char.

Small bands observed in regions 1140–1000 cm^{-1}, 1620–1450 cm^{-1} and 1700 cm^{-1} FTIR spectra (Supplementary material, Fig. S1) were assigned to ether, quinone and lactonic groups [28]. Those three bands on the spectrum of acid treated activated char were more intense than activated char, suggesting that the acid

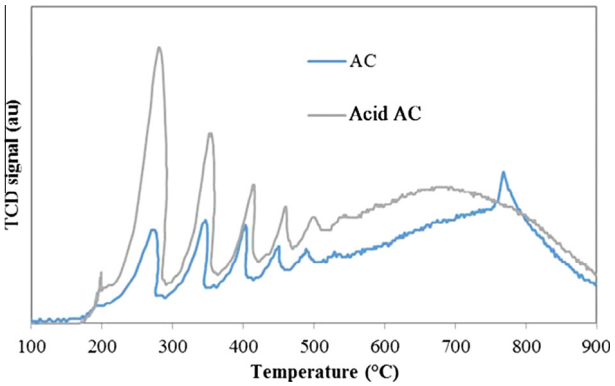

Fig. 2. TPD profiles of raw activated char and acid treated activated char.

treated activated char contained higher amounts of ether, quinone and lactonic groups than the activated char. The observation of higher quinone groups was consistent with results from TPD.

3.1.3. X-ray Diffraction (XRD)

One broad peak at 23° and one weak peak at around 43° were observed on the activated char (Supplementary material, Fig. S1). The peak at 23° was attributed to the (0 0 2) reflection of the graphitic-type lattice and the peak at 43° corresponded to a superposition of (1 0 0) and (1 0 1) reflections of the graphitic-type lattice. The broadness and weakness of two reflection peaks of activated char indicated a low degree of graphitization. The XRD patterns of the Ni-AC-A and Ni-AC-AH showed three reflection peaks (Supplementary material, Fig. S1) at 44.5° and 51.5° and 76.4°. Those peaks were assigned to crystal planes of 111, 200 and 220 of metallic nickel with a face-centered cubic structure [13]. The spectrum signals of Ni-AC-AH were less intense than that of Ni-AC-A, suggesting a smaller nickel particle size and better metal dispersion on Ni-AC-AH. XRD pattern of Ni-AC-N only showed two peaks at 44.5° and 51.5°. Both peaks were less intense than XRD peaks of Ni-AC-AH and Ni-AC-A, suggesting that Ni-AC-N had the highest nickel dispersion and smallest nickel particle size. The nickel crystal sizes of Ni-AC-A and Ni-AC-AH were estimated (see Table 1) using the Scherrer equation through line broadening at half the maximum intensity of the most intense peak. The estimation of nickel crystal size of Ni-AC-N was not possible due to difficulty in obtaining the line broadening at half the maximum intensity of the most intense peak.

Activated carbon showed only one XRD peak associated with minerals and that peak corresponded to Nickel. The peaks associated with inherent minerals of biochar were not visible because of the negligible concentrations of minerals in the prepared activated carbon. The contents of Ca, K and Mg (three most abundant metallic minerals) in raw eastern redcedar char were 3.91 wt.%, 0.23 wt.% and 0.14 wt.%, respectively. During preparation of the activated carbon, these inherent minerals were washed out. Many studies have reported that the inherent minerals did play catalytic role during biomass pyrolysis and gasification. However, considering the low/unnoticeable contents of minerals in prepared activated carbon and high contents of nickel (10 wt.%), the catalytic effect of the inherent minerals on tar reforming is considered insignificant compared to that of nickel.

3.1.4. TEM

As shown in Fig. 3, the shape of the nickel particles on the three catalysts was essentially spherical. Ni-AC-N (Fig. 3(a)) showed the highest nickel dispersion and smallest particle sizes, which was consistent with the results obtained from XRD. The nickel particle size of Ni-AC-A (Fig. 3(b)) was larger and agglomeration of nickel particles was more severe, while the nickel particle of Ni-AC-AH (Fig. 3(c)) dispersed better and was smaller, indicating hydrazine treatment improved the metal dispersion on catalyst with nickel

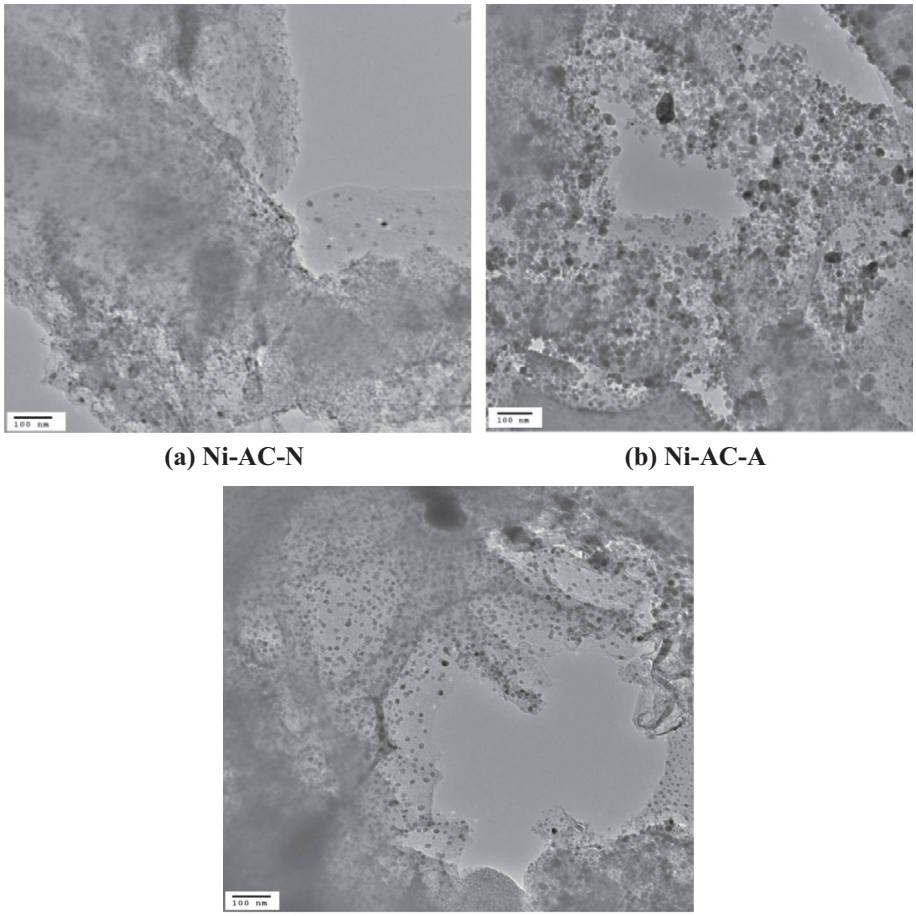

(a) Ni-AC-N (b) Ni-AC-A

(c) Ni-AC-AH

Fig. 3. TEM of activated char supported nickel catalysts.

acetate precursor. The same phenomenon was also observed by Wojcieszak et al. [13]. While preparing activated char supported nickel catalysts for benzene hydrogenation, they found that the nickel catalysts prepared by hydrazine chemical reduction had much smaller particle size (<5 nm) than that prepared by hydrogen reduction methods (10–40 nm). The nickel particles sizes of Ni-AC-N, Ni-AC-A and Ni-AC-AH measured from TEM were 7–13, 15–39 and 11–18 nm, respectively (Table 1).

3.2. Catalyst activity

3.2.1. Steam reforming of toluene

3.2.1.1. Influence of reforming temperature and catalyst on toluene removal. It can be seen that the reforming temperature significantly influences toluene conversion. Nickel precursor also greatly affected toluene conversion (see Fig. 4). Catalyst prepared from nickel nitrate precursor (Ni-AC-N) showed the highest toluene conversion (72% and 80% at 600 and 700 °C, respectively), whereas catalysts prepared from nickel acetate (Ni-AC-A and Ni-AC-AH) showed lower toluene conversion (58% and 65% for Ni-AC-A, 63% and 72% for Ni-AC-AH). The lower activity of the catalysts prepared from nickel acetate than the catalyst prepared from nickel nitrate was probably due to lower dispersion and larger metal nickel particle sizes as seen from the results of XRD and TEM. The lower catalyst activity was also probably due to the incomplete reduction of nickel acetate. Wojcieszak et al. [29] found that the catalyst with nickel acetate precursor was more difficult to reduce than the catalyst with nickel nitrate precursor. The nickel acetate precursor was not completely reduced by hydrogen at temperature below 733 K while the nickel nitrate catalyst could be easily reduced into metal nickel (Ni^0, metallic state) at 623 K [29]. The nickel nitrates precursor was able to reduce at such low temperature because nickel nitrates species could easily be calcined into NiO even at low temperature (500 K) [9].

Performances of various catalysts in steam reforming of toluene as model tar have been studied (Table 2) and different tar removing efficiencies have been reported. The efficiency of Ni-AC-N was close to other nickel catalysts reported in literature [23,30]. However, the efficiency of Ni-AC-A was lower than those reported. However, direct comparison of different catalysts as reported in different studies may not be reasonable, because reforming conditions, such as steam to carbon ratio and space time, were different. Those conditions were proven to affect catalyst performance. For instance, two space times were used to test activity of three commercial catalysts (Cerium zirconium platinum, Hifuel R110 and Reformax 250) by Mudinoor et al. [31] and the results showed that high space velocity heavily enhanced the catalysts' efficiency.

3.2.1.2. Gas composition and benzene yield of steam reforming of toluene. Various reactions mechanisms have been hypothesized in literatures during toluene reforming and are summarized as follows [23,32]:

$$\text{Steam reforming}: \quad C_7H_8 + 7H_2O \rightarrow 7CO + 11H_2 \tag{4}$$

$$C_7H_8 + 14H_2O \rightarrow 7CO_2 + 18H_2 \tag{5}$$

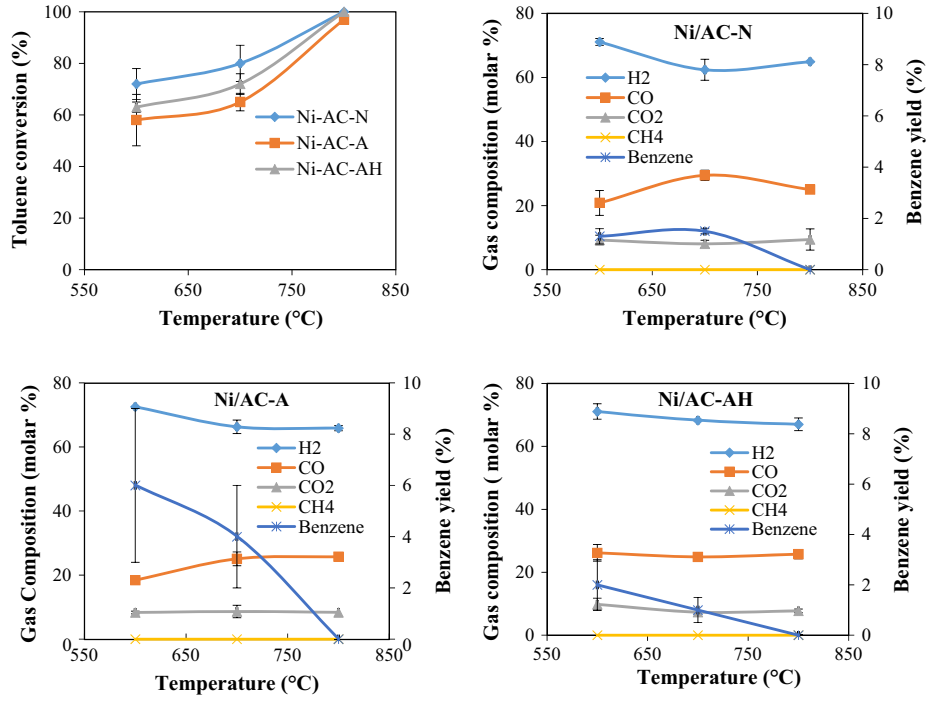

Fig. 4. Toluene conversion and gas compositions for steam reforming of toluene with three catalysts at 600–800 °C (dry and nitrogen free basis).

Table 2
Catalytic performance of different catalysts reported in literatures.

Catalyst	Temperature (°C)	Space time (kg_{cat} h/m^3)	Toluene conversion (%)	Reference
Ni/olivine	600–850	9[a]	74–100	[23]
Ni-CeO_2/SBA-15	700–850	16[a]	80–99	[30]
Cerium zirconium platinum	700	7.5E−4–1.26E−3[b]	70–95	[31]
Hifuel R110	700	7.5E−4–1.26E−3[b]	80–97	[31]
Reformax 250	700	7.5E−4–1.26E−3[b]	75–93	[31]

[a] Defined as the catalyst weight over the volumetric flow rate of toluene vapor.
[b] Defined as the catalyst weight over the volumetric flow rate of total gas flow.

Water gas shift : $CO + H_2O \leftrightarrow CO_2 + H_2$ (6)

Dry reforming : $C_7H_8 + 7CO_2 \rightarrow 14CO + 4H_2$ (7)

Hydrodealkylation : $C_7H_8 + H_2 \rightarrow C_6H_6 + CH_4$ (8)

Methane steam reforming : $CH_4 + H_2O \rightarrow CO + 3H_2$ (9)

Water gas reaction : $C + H_2O \leftrightarrow CO + H_2$ (10)

Boudouard reaction : $C + CO_2 \leftrightarrow 2CO$ (11)

As shown in Fig. 4, low benzene yield was observed at all conditions (Null-2%), except for Ni-AC-A catalyst at 600 and 700 °C (4–9%). For all catalysts, benzene yield decreased as the reaction temperature increased from 600 to 800 °C. The decrease in benzene yield was probably because high temperature promoted the decomposition of benzene into permanent gases. Benzene is more thermally stable than toluene and its decomposition requires more energy [33].

The primary gas product of steam reforming of toluene was H_2 followed by CO and CO_2 (see Fig. 4). CH_4 was not detected in any experiments. The absence of CH_4 in the final products indicated that CH_4, as an intermediate of hydrodealkylation reaction, was consumed by methane steam reforming. The H_2 and CO_2 decreased as the temperature increased from 600 to 700 °C while the CO increased with decrease in temperature. This might be caused by the improved endothermic reverse water gas shift reaction (Eq. (9)) at high temperature [30]. This trend was also reported by Tao et al. [30] during steam reforming of toluene over Ni/SBA-15 catalyst. Since H_2 and CO can potentially generate from either reaction of steam with activated carbon or toluene, a control experiment at 700 °C with steam was performed to compare H_2 and CO/CO_2 yields from toluene with the activated carbon catalyst and from the activated carbon catalyst (no toluene). Results showed that H_2 and CO/CO_2 yields from only activated carbon catalyst (no toluene) were negligible as compared to those from toluene with the activated carbon catalyst. This implies that toluene reforming was the major reaction that contributed to the production of H_2, CO and CO_2. However, the carbon support with nickel loading have found to react with hydrogen [13] and results of this study have also shown indicated that the carbon support was partly converted into gaseous form.

3.2.2. Steam reforming of naphthalene/toluene

3.2.2.1. Catalyst activity for steam reforming of naphthalene/toluene. Because Ni-AC-N was found to be the most effective in steam reforming of toluene, Ni-AC-N was selected as the catalyst

for steam reforming of naphthalene/toluene. The results of toluene and naphthalene steam reforming are shown in Fig. 5. At temperature below 900 °C, the conversions of toluene and naphthalene were similar. At 900 °C, the conversion of toluene was significantly higher than that of naphthalene. Increase in temperature significantly increased reforming efficiencies of both toluene and naphthalene: the toluene conversion increased from 36% to 99% and naphthalene conversion increased from 37% to 92% as temperature increased from 700 to 900 °C.

The reforming efficiency of toluene only was significantly higher than that of naphthalene/toluene. The conversion of toluene was 87% at 700 °C, while conversion was only 36% for naphthalene/toluene reforming. This indicated that steam reforming of toluene in naphthalene/toluene was more difficult than steam reforming of toluene alone. This phenomena was also found by Jess [34] during catalytic reforming of naphthalene and benzene in the presence of hydrogen and steam. Jess found that the conversion of benzene during catalytic reforming of benzene/naphthalene was significantly lower than conversion of benzene only (no naphthalene). The decrease of benzene removal efficiency in the presence of naphthalene was explained as follows: the adsorption of naphthalene on the surface of the catalyst occurred strongly, thereby decreasing the conversion of benzene. Benzene adsorbed only weakly and thus did not influence the catalytic conversion. For this study, temperature below 900 °C, naphthalene did not completely reform and the unconverted naphthalene strongly adsorbed on the surface of the catalyst. As a result, adsorbed naphthalene might have covered the active sites on catalyst and affected the reforming efficiency.

3.2.2.2. Gas composition and benzene yield of steam reforming of naphthalene/toluene. Benzene yield and product gas composition are presented in Fig. 5. The benzene yields were very low (less than 3%) and decreased with temperature. The benzene yield of naphthalene/toluene reforming was slightly higher than that of toluene (0–1% at 600–800 °C). In the product gas, H_2 was the main component at all temperatures followed by CO and CO_2. The amount of CH_4 was unnoticeable at all temperatures. H_2 molar composition was the highest at 700 °C and kept nearly constant at 800–900 °C (65% at 800 °C and 66% at 900 °C). Similar to H_2, the composition of CO_2 was the highest at 700 °C and held nearly constant at 800–900 °C. The CO composition showed a different trend with respect to temperature as compared to H_2 and CO_2. CO composition was the lowest (13%) at 700 °C and the highest at 800 °C (28%).

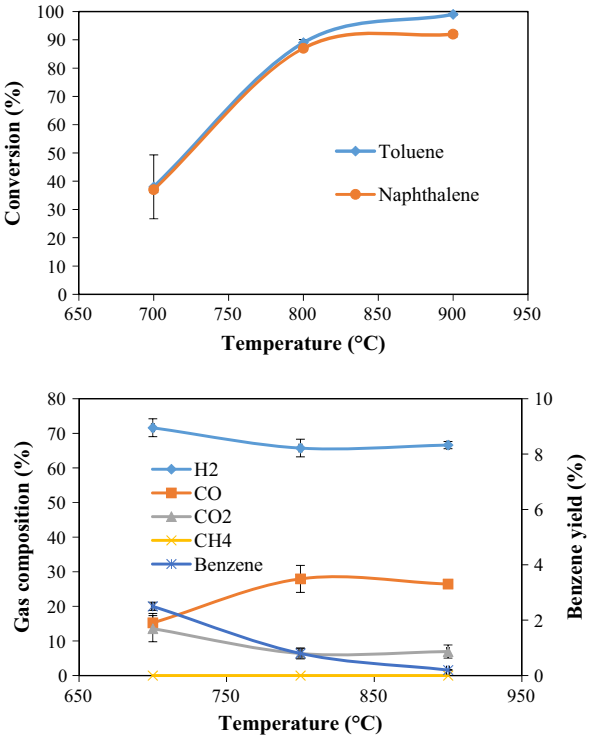

Fig. 5. Naphthalene and toluene conversions and compositions of gas for steam reforming of naphthalene/toluene with Ni-AC-N at 700–900 °C.

Zhao et al. [35] performed thermodynamic analysis on steam reforming of toluene with different steam to carbon ratios (1.0–4.0) and temperatures (650–1500 °C). Their calculation was based on equivalent reaction described in literature [27,35]. Trends of H_2, CO_2 and CO with respect to temperature based on thermodynamic equilibrium was different from the trends obtained in this study's experimental data. H_2 held almost constant at all temperatures based on the thermodynamic equilibrium while it was the highest at 700 °C in our experimental results. CO composition almost linearly increased with temperature based on thermodynamic equilibrium while it was first increased then decreased with temperature. CO_2 decreased with temperature and was at highest at 700 °C. Similar to the absence of methane in this study, methane was absent in thermodynamic equilibrium results. The difference in gas composition between the results of thermodynamic equilibrium study and this experiment indicates that steam reforming of naphthalene/toluene over a char based catalyst is more complicated than the equivalent reaction described [27,35].

3.3. Used catalyst characterization

The used Ni-AC-N was characterized by nitrogen adsorption and SEM. Total surface area, total pore volume and micropore volume of the used Ni-AC-N are listed in Table 1. The surface area of the used catalyst (265 m^2/g) was significantly lower than that of the fresh catalyst (965 m^2/g). The used catalyst was primarily composed of mesopores (59%) followed by micropores (22%) and macropores (19%).

The morphologies of the activated char, fresh and used catalyst were examined by Scanning Electron Microscopy (SEM). As shown in SEM images of activated char and the fresh catalysts (Fig. 6(a) and (b)), we can still see the basic fibrous structure of the red cedar. The micropores (<2 nm) on activated char was too small to be seen due to the limitation on SEM resolution. On the images of the used catalyst (Fig. 6(c)), structural damage seemed to occur on the activated char support. This resulted from coking [32] and thermal degradation of the catalysts. As discussed earlier, the carbon support was also found to react with methane when nickel was present in the catalyst, resulting in thermal degradation and structural damage to the carbon support. The char support may also react with CO_2 and steam at the reaction temperature (600–900 °C). The structural destruction of the used catalyst may have caused destruction of micropore structure of the activated char and thus leading to significant decreases in surface area and pore volume of micropores (see Table 1).

Fig. S3 (Supplementary material) showed the backscattered image of fresh catalyst and used catalyst. Only a very small amount of supported nickel appeared to scatter on the surface of fresh catalyst, since most of the nickel was impregnated in the pores of activated char. In comparison, a large portion of nickel particles appeared to disperse on the surface of the used catalyst. This was probably because of the exposure of the impregnated nickel due to the structural destruction of the activated char support during reforming.

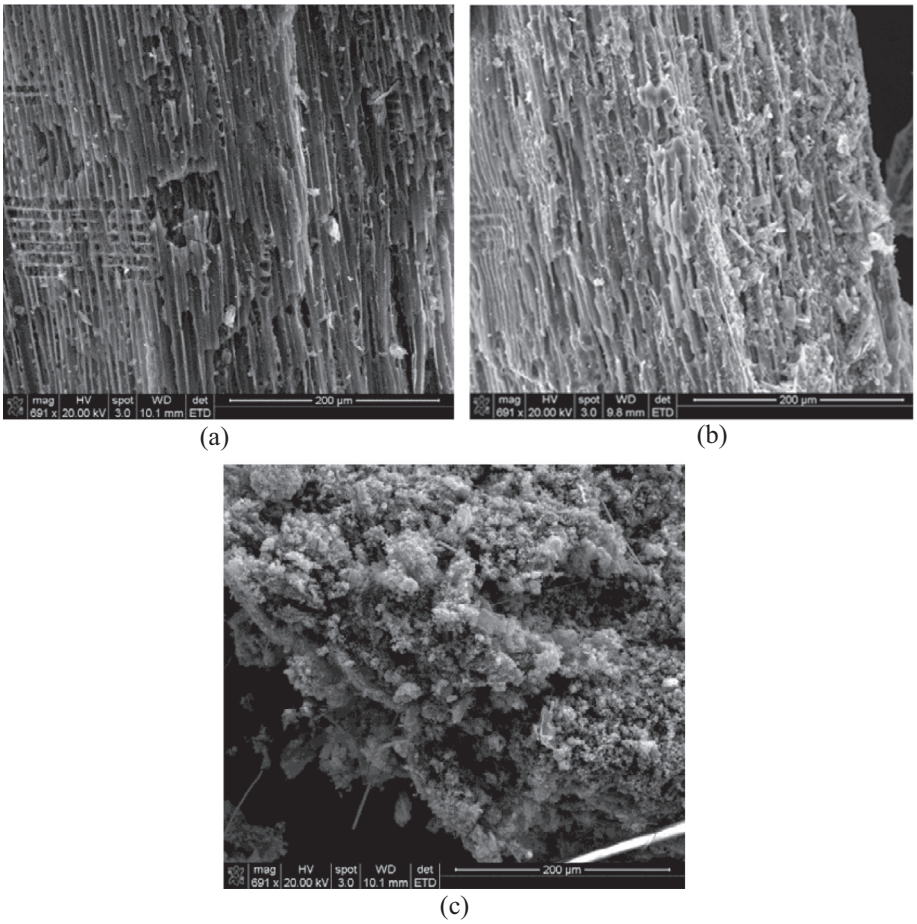

Fig. 6. Scanning electron microscopy (SEM) images of (a) activated char, (b) fresh catalyst and (c) used catalyst.

4. Conclusions

The catalytic efficiency of toluene removal for the three catalysts was ranked from the highest to the lowest as Ni-AC-N > Ni-AC-AH > Ni-AC-A. Nickel particle size of the catalyst impregnated with nickel nitrate (Ni-AC-N) was smaller than that of catalyst impregnated with nickel acetate (Ni-AC-A and Ni-AC-AH). The particle size of catalyst impregnated with nickel acetate decreased with hydrazine reduction but was still larger than catalyst impregnated with nickel nitrate. Steam reforming of naphthalene/toluene showed that toluene had higher removal efficiency than naphthalene. The presence of naphthalene decreased the toluene removal. TPR and SEM results indicated that the char based catalyst was prone to react during steam reforming.

Acknowledgement

This material is based upon work that is supported by the National Institute of Food and Agriculture, U.S. Department of Agriculture, through South Central Sun Grant Program.

Appendix A. Supplementary material

Supplementary data associated with this article can be found, in the online version, at http://dx.doi.org/10.1016/j.fuel.2016.09.043.

References

[1] Anis S, Zainal ZA. Tar reduction in biomass producer gas via mechanical, catalytic and thermal methods: a review. Renew Sust Energy Rev 2011;15:2355–77.
[2] Milne TA, Evans RJ. Biomass gasifier "tars": their nature, formation, and conversion, in. Golden Colorado: National Renewable energy laboratory; 1998.
[3] Abu El-Rub Z, Bramer EA, Brem G. Review of catalysts for tar elimination in biomass gasification processes. Ind Eng Chem Res 2004;43:6911–9.
[4] Rapagnà S, Gallucci K, Di Marcello M, Matt M, Nacken M, Heidenreich S, et al. Gas cleaning, gas conditioning and tar abatement by means of a catalytic filter candle in a biomass fluidized-bed gasifier. Bioresour Technol 2010;101:7123–30.
[5] Wang L, Li D, Koike M, Watanabe H, Xu Y, Nakagawa Y, et al. Catalytic performance and characterization of Ni–Co catalysts for the steam reforming of biomass tar to synthesis gas. Fuel 2013;112:654–61.
[6] Van Der Laan GP, Beenackers AACM. Kinetics and selectivity of the fischer-tropsch synthesis: a literature review. Catal Rev 1999;41:255–318.
[7] Abu El-Rub Z, Bramer EA, Brem G. Experimental comparison of biomass chars with other catalysts for tar reduction. Fuel 2008;87:2243–52.
[8] Zheng X, Zhang S, Xu J, Wei K. Effect of thermal and oxidative treatments of activated carbon on its surface structure and suitability as a support for barium-promoted ruthenium in ammonia synthesis catalysts. Carbon 2002;40:2597–603.
[9] Domingogarcia M, Fernandezmorales I, Lopezgarzon FJ. Activated carbons as supports for nickel-catalysts. Appl Catal A – Gen 1994;112:75–85.
[10] Abotsi GMK, Scaroni AW. A review of carbon-supported hydrodesulfurization catalysts. Fuel Process Technol 1989;22:107–33.
[11] Molina-Sabio M, Pérez V, Rodríguez-Reinoso F. Impregnation of activated carbon with chromium and copper salts: effect of porosity and metal content. Carbon 1994;32:1259–65.
[12] Aksoylu AE, Madalena M, Freitas A, Pereira MFR, Figueiredo JL. The effects of different activated carbon supports and support modifications on the properties of Pt/AC catalysts. Carbon 2001;39:175–85.
[13] Wojcieszak R, Zieliński M, Monteverdi S, Bettahar MM. Study of nickel nanoparticles supported on activated carbon prepared by aqueous hydrazine reduction. J Colloid Interf Sci 2006;299:238–48.

[14] Li H, Yu D, Hu Y, Sun P, Xia J, Huang H. Effect of preparation method on the structure and catalytic property of activated carbon supported nickel oxide catalysts. Carbon 2010;48:4547–55.
[15] Guo JX, Liang J, Chu YH, Sun MC, Yin HQ, Li JJ. Desulfurization activity of nickel supported on acid-treated activated carbons. Appl Catal A – Gen 2012;421–422:142–7.
[16] Xie Q, Zhang XL, Chen QR, Gong GZ. Influence of surface modification by nitric acid on the dispersion of copper nitrate in activated carbon. New Carbon Mater 2003;18:203–8.
[17] Boudjahem AG, Monteverdi S, Mercy M, Bettahar MM. Study of nickel catalysts supported on silica of low surface area and prepared by reduction of nickel acetate in aqueous hydrazine. J Catal 2004;221:325–34.
[18] Bettahar MM, Wojcieszak R, Monteverdi S. NiAg catalysts prepared by reduction of Ni^{2+} ions in aqueous hydrazine: II. Support effect. J Colloid Interf Sci 2009;332:416–24.
[19] Shen Y, Yoshikawa K. Recent progresses in catalytic tar elimination during biomass gasification or pyrolysis—a review. Renew Sust Energy Rev 2013;21:371–92.
[20] Michel R, Łamacz A, Krzton A, Djéga-Mariadassou G, Burg P, Courson C, et al. Steam reforming of α-methylnaphthalene as a model tar compound over olivine and olivine supported nickel. Fuel 2013;109:653–60.
[21] Guan G, Chen G, Kasai Y, Lim EWC, Hao X, Kaewpanha M, Abuliti A, Fushimi C, Tsutsumi A. Catalytic steam reforming of biomass tar over iron- or nickel-based catalyst supported on calcined scallop shell. Appl Catal, B: Environ 2012;115–116:159–68.
[22] Liu H, Chen T, Zhang X, Li J, Chang D, Song L. Effect of additives on catalytic cracking of biomass gasification tar over a nickel-based catalyst. Chin J Catal 2010;31:409–14.
[23] Świerczyński D, Libs S, Courson C, Kiennemann A. Steam reforming of tar from a biomass gasification process over Ni/olivine catalyst using toluene as a model compound. Appl Catal, B: Environ 2007;74:211–22.
[24] Patil K, Bhoi P, Huhnke R, Bellmer D. Biomass downdraft gasifier with internal cyclonic combustion chamber: design, construction, and experimental results. Bioresour Technol 2011;102:6286–90.
[25] Hsu LY, Teng H. Influence of different chemical reagents on the preparation of activated carbons from bituminous coal. Fuel Process Technol 2000;64:155–66.
[26] Moreno-Castilla C, Carrasco-Marın F, López-Ramón MV, Alvarez-Merino MA. Chemical and physical activation of olive-mill waste water to produce activated carbons. Carbon 2001;39:1415–20.
[27] Josuinkas FM, Quitete CPB, Ribeiro NFP, Souza MMVM. Steam reforming of model gasification tar compounds over nickel catalysts prepared from hydrotalcite precursors. Fuel Process Technol 2014;121:76–82.
[28] Lagos G, García R, Agudo AL, Yates M, Fierro JLG, Gil-Llambías FJ, et al. Characterisation and reactivity of Re/carbon catalysts in hydrodesulphurisation of dibenzothiophene: effect of textural and chemical properties of support. Appl Catal A – Gen 2009;358:26–31.
[29] Wojcieszak R, Zielinski M, Monteverdi S, Bettahar MM. Study of nickel nanoparticles supported on activated carbon prepared by aqueous hydrazine reduction. J Colloid Interf Sci 2006;299:238–48.
[30] Tao J, Zhao L, Dong C, Lu Q, Du X, Dahlquist E. Catalytic steam reforming of toluene as a model compound of biomass gasification tar using Ni-CeO_2/SBA-15 catalysts. Energies 2013;6:3284–96.
[31] Mudinoor A, Bellmer D, Marin L, Kumar A, Huhnke R. Conversion of toluene (model tar) using selected steam reforming catalysts. Trans ASABE 2011;54:1819–27.
[32] Bhandari PN, Kumar A, Bellmer DD, Huhnke RL. Synthesis and evaluation of biochar-derived catalysts for removal of toluene (model tar) from biomass-generated producer gas. Renew Energy 2014;66:346–53.
[33] Kong M, Yang Q, Fei J, Zheng X. Experimental study of Ni/MgO catalyst in carbon dioxide reforming of toluene, a model compound of tar from biomass gasification. Int J Hydrogen Energy 2012;37:13355–64.
[34] Jess A. Catalytic upgrading of tarry fuel gases: a kinetic study with model components. Chem Eng Process 1996;35:487–94.
[35] Zhao B, Zhang X, Chen L, Qu R, Meng G, Yi X, et al. Steam reforming of toluene as model compound of biomass pyrolysis tar for hydrogen. Biomass Bioenergy 2010;34:140–4.